Available online at www.sciencedirect.com

SciVerse ScienceDirect

Energy Procedia 21 (2012) 84 – 91

Energy Procedia

3rd Workshop on Metallization for Crystalline Silicon Solar Cells,

25 – 26 October 2011, Charleroi, Belgium

Long-term stable encapsulated solder joints on an Al/Ni:V/Ag metallization for silicon solar cells

Verena Jung, Frank Heinemeyer*, Marc Köntges

Institute for Solar Energy Research Hamelin (ISFH), Am Ohrberg 1, 31860 Emmerthal, Germany

Abstract

Evaporated Al as metallization for silicon solar cells may be profitable as it requires less Al material than the common screen-printed Al/Ag-paste combinations and forms contacts with a lower contact resistivity. To achieve solderability a sputter deposited Ni:V and an Ag layer are deposited onto the evaporated Al layer. Tin-coated Cu-connectors with a lead-free and a lead-containing solder are employed in combination with two halogen-free no-clean fluxes with varying solid contents. The long-term solderability of the metallization stack is demonstrated by comparing 180° peel forces (DIN EN 50461) of Cu-connectors soldered onto the metallization stack directly after preparation, after accelerated storing following IPC J-STD-003B and after storing for half a year at room temperature. The long-term stability of the solder joints is verified by measuring the normalized contact resistivity and by a visual inspection of encapsulated samples during a damp heat test (DIN EN 61215). For encapsulation an EVA foil and a silicone elastomer are used as encapsulation materials. As the lead-containing solder does not adhere sufficiently after accelerated aging, the flux with high contend of solids may accelerate corrosion and the EVA laminates exhibit adhesion problems between the samples and the lamination foil. The lead-free solder and the flux with the lower solid content in a silicone elastomer based laminate emerge to be the most promising candidates for a long term stable interconnection of Al/Ni:V/Ag metallized solar cells.

© 2012 Published by Elsevier Ltd. Selection and/or peer review under responsibility of Guy Beaucarne
Open access under CC BY-NC-ND license.

Keywords: crystalline silicon; solar cell; metallization; long-term stable; solder joint; laminate; evaporation; sputtering;

1. Introduction

Aluminum is a well known metallization for silicon solar cells. For standard screen printed solar cells

* Corresponding author. Tel.: +49 (0)5151 999 416; Fax: +49 (0)5151 999 400.
E-mail address: heinemeyer@isfh.de.

1876-6102 © 2012 Published by Elsevier Ltd. Selection and/or peer review under responsibility of Guy Beaucarne
Open access under CC BY-NC-ND license. doi:10.1016/j.egypro.2012.05.011

it is introduced as porous Al paste and combined with solder pads consisting of a solderable Ag paste [1]. Related to the Al weight, evaporated Al requires only about 10% of the amount of screen printed Al paste and may thus be more profitable [2-4]. To obtain a solderable surface a sputtered Ni:V layer and a subsequently sputtered Ag layer are deposited on the evaporated Al layer [5]. This metallization stack is adapted from microelectronics, known there as under bump metallization (UBM) [6-8]. Fig. 1 shows a SEM cross section of an Al/Ni:V/Ag metallization stack on a Si wafer.

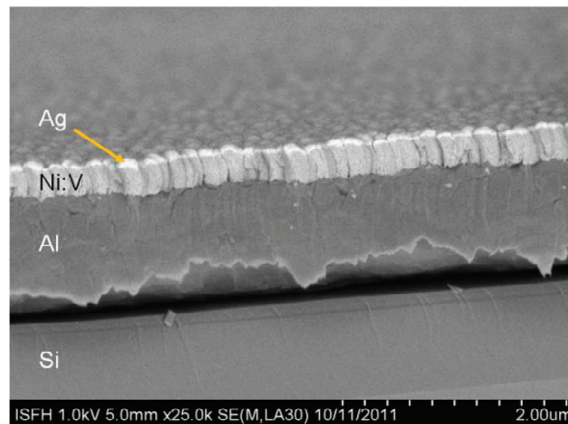

Fig. 1. Metallization stack on silicon wafer: 1 µm evaporated Al (dark grey with breaking edge in the bottom of the layer), 250 nm sputtered Ni:V (light grey) and 25 nm sputtered Ag (white)

For the preparation of a PV module the solar cells need to be interconnected and encapsulated in a laminate. In a standard PV module ethylen vinyl acetate (EVA) and a Tedlar based foil are the common encapsulation foil and back sheet [9]. For the interconnection of the solar cells a solder and a flux need to be selected. As the three metal layers Al, Ni:V and Ag are vacuum deposited on top of each other, the resulting surface is much more flat and less oxidized compared to the surface of a screen printed and fired Al and Ag paste. Consequently all materials and processes belonging to the module preparation need to be tested in combination with the vacuum deposited metallization. The aim of this work is to demonstrate the long-term solderability of a vacuum deposited Al/Ni:V/Ag metallization. Secondly, the best working combination of a solder, a flux and an encapsulation material for the preparation of PV modules based on this metallization is determined and the long-term stability of encapsulated solder joints is verified.

2. Experimental

After cleaning, the test wafers (125 × 125 mm² Cz-grown Si) are metallized in an in-line high-rate metallization system (ATON from Applied Materials) [3]. The metallization stack consisting of 2 µm evaporated Al and 200 nm sputtered Ni:V as well as 25 nm sputtered Ag is deposited. All deposition steps are carried out without vacuum break.

2.1. Setup of storage test

The storage test was realized with 12 samples, split up in three groups with four different solder/flux combinations in each group. The first group, shown in Fig. 2 as “3.a Direct processing” was soldered directly after metallization, simulating an integrated industrial production process of wafers and modules.

The second group ("3.b Accelerated storage") is soldered after accelerated storing following IPC J-STD-003B. This norm test includes 8 h storage at 72°C and 85% relative humidity followed by 1 h storage at 105°C and is carried out to simulate half a year of storage time. The last four samples of the third group ("3.c Storage") are stored at room temperature for half a year before soldering to check if storing of the solar cells after production is possible for this industrial relevant duration.

In each group we use four different solder/flux combinations. The Cu-connectors used here are fabricated by roll cladding of copper plates with a lead-free solder consisting of 96.5 wt% Sn and 3.5 wt% Ag or a lead-containing solder comprising 62 wt% Sn, 36 wt% Pb and 2 wt% Ag. The connectors are soldered onto the metalized samples using halogen-free no-clean fluxes, either with a high (959T from Kester) or with a low solid content (952S from Kester). The solder/flux combinations are shown in Fig. 2 "4. Soldering".

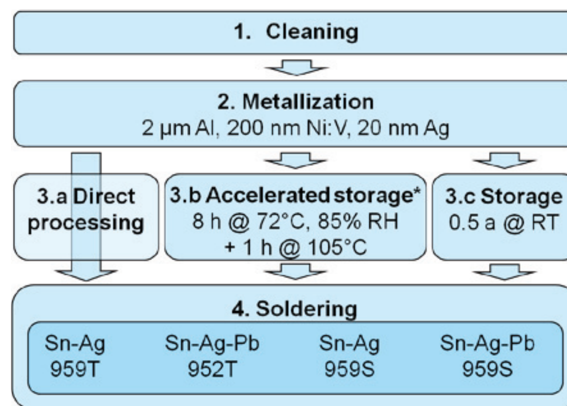

Fig. 2. Schematic representation of sample preparation for 180° peel test

To test the solderability of metallized wafers, stored for different times, a 180° peel test (according to DIN EN 50461) was carried out. Therefore, wafer with solder joints are cut in 2 x 12.5 cm² samples using an infrared ns laser system. This samples were investigated in a solar cell peel tester from Zwick to peel the connector off in an angle of 180°. During the peel test a force-path is measured for each peeled off connector. From the force-path measurements the maximum peel force F_{max}, the mean peel force F_{mean} and the minimum peel force F_{min} are determined excluding 50 mm at the start and the end of the measurement. For an acceptable mechanical contact all measured peel forces must be above 1 N/mm. For screen printing pastes the cohesion fracture is expected to be in the screen printing paste, because the paste is the weakest layer. In contrast for evaporated metallizations as used in this work the cohesion fracture is expected to be in the solder. In this metallization stack the solder is the weakest layer. To high forces during soldering lead to micro-cracks in the silicon wafer. In the peel test this micro-cracks cause spalling of the silicon. Hence, indicating suitable soldering forces, no spalling of silicon parts must occur.

2.2. Setup for long-term stability test of solder joints

In order to investigate the long-term stability of the solder joints we carry out a 2000 h damp heat test. Damp heat is the most corrosive test for solder joints within the EN 61215 norm, used for stability tests of modules in the PV industry. In this test we used also the solder/flux combinations described in the

previous paragraph. Soldering is carried out directly after metallization without any storage of the samples (see Fig. 3, “3.a Soldering without storage”). To assess the resulting corrosion of the solder joints, visual inspections and contact resistivity (R_C) measurements using the transfer length method (TLM) are carried out after 0, 125, 250, 500, 1000, and 2000 h test duration in the damp heat test. For each solder/flux combination two TLM arrays were prepared on one wafer as shown in Fig. 4.

Due to lamination of the contact area on the wafer, the transfer length resistance is measured at the end of the connectors in between the damp heat test. This leads to an additional resistance depending on the length of the connector. To eliminate this additional resistance, we measured the initial contact resistivity $R_{C.in}$ directly on the contacts and set this value to 1.00. A second measurement takes place at the end of the connectors. The difference of initial contact resistance and resistance measured at the end of the connectors gives the bias resistance caused by the connector cable. This value has to be subtracted from measured transfer length resistances in the damp heat test to get the corrected contact resistivity R_C. Two TLM arrays are used for averaging of R_C and $R_{C.in}$. We define the normalized contact resistivity as $R_C/R_{C.in}$.

For the lamination of the TLM samples three different kinds of laminates are used. Fig.3, 4A + 4B shows two laminates prepared in a conventional configuration with two different lamination foils and a tedlar backsheet to test the influence of the lamination material. Laminate A (“EVA”) consists of a glass/EVA/samples/EVA/Tedlar and laminate B (“Tectosil”) of glass/Tectosil/samples/Tectosil/Tedlar stack. The third laminate C is prepared as “open” sample without backsheet and consists of glass/EVA/samples/EVA. This enables the visual inspection of the contacts and a more aggressive impact of the damp heat test. For preparation of the samples we use Tectosil 177, a silicon elastomer fabricated by Wacker, EVA 49610 from Etimex and Tedlar 2442 Icosolar 0,35 from Isovolta.

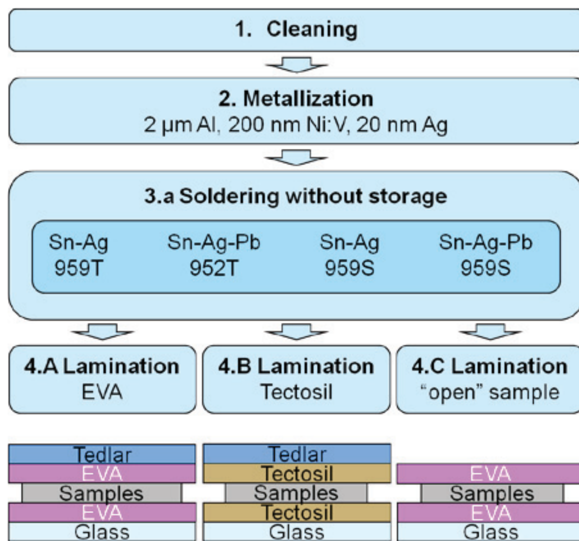

Fig. 3. Schematic representation of sample preparation for damp heat test

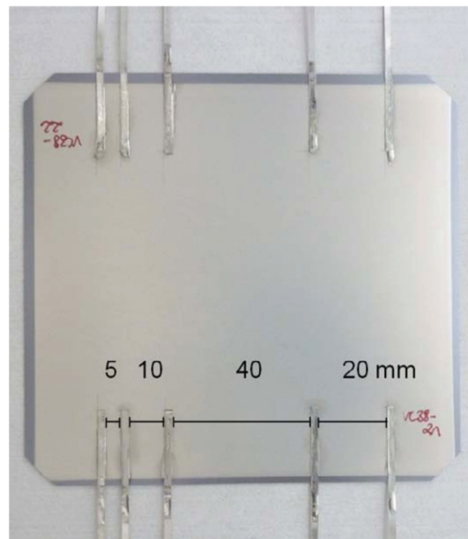

Fig. 4. Sample preparation for normalized contact resistivity measurements with the transfer length method

3. Results

3.1. Results of storage test

In Fig. 5 the measured peel forces from the storage test are plotted as function of the solder/flux combination. If the samples are soldered directly after preparation of the metallization stack, the minimum peel force F_{min} is larger than 1 N/mm for all solder/flux combinations as it is required in the DIN EN 50461. In Fig. 5 (a) it is also shown, that the mean peel force F_{mean} is larger than 5 N/mm except for the lead-containing solder joint with the low solid-content flux. In Fig. 5 (b) we present the results after accelerated storage of the metallized Si-wafers. Samples with the Sn-Ag solders reveal a minimum peel force F_{min} being still larger than 3-5 N/mm. For the lead-containing samples the minimum peel force decreases and varies between 0.5 and 1 N/mm. Fig. 5 (c) shows the results after storage for 0.5 a at room temperature. The minimum peel force F_{min} for the Sn-Ag solders varies again between 3 and 5 N/mm and is about 1 N/mm for the Sn-Ag-Pb solders. Looking at Fig. 5 (b) and (c), the peel forces after accelerated storage of the metallization according to IPC J-STD-003B and after storage half a year are comparable. The application of the Sn-Ag-Pb solders especially in combination with the flux 952S is critical as its minimum peel forces are about or smaller than 1 N/mm. The cohesion fracture is for all tested samples as expected in the solder. We did not find spalling in all tests.

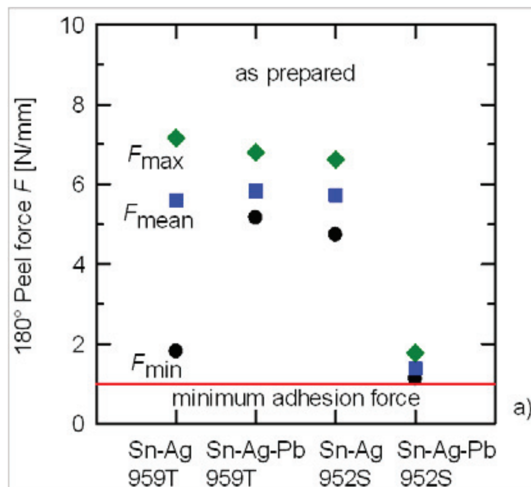

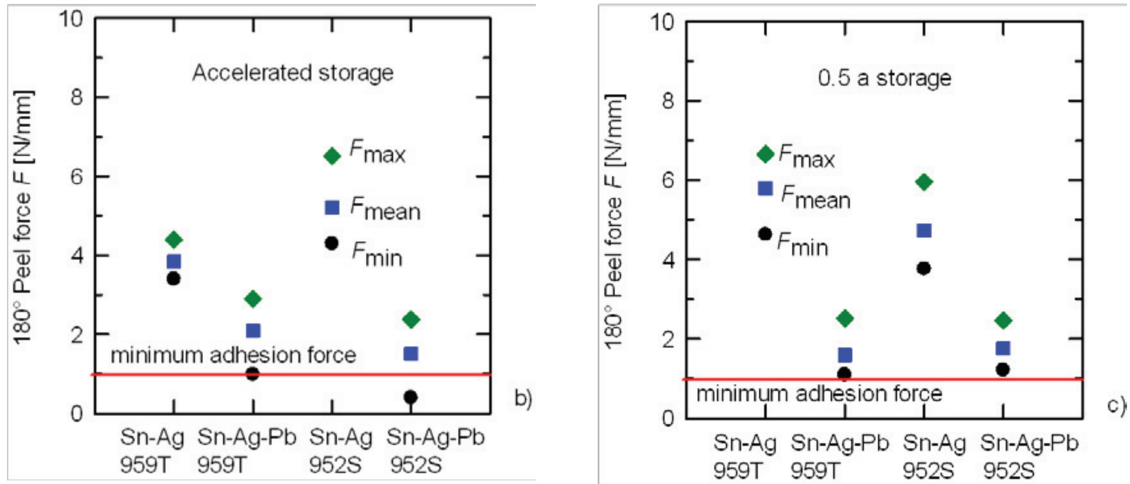

Fig. 5. Minimum, mean and maximal 180° peel force as function of solder and flux of the solder joint. The soldering is performed (a) as prepared, (b) after accelerated storage and (c) after 0.5 a storage of the metallized samples. The red line labeled "minimum adhesion force" shows the required minimum peel force according to DIN EN 50461.

3.2. Results of accelerated aging

The visual inspection of the test modules reveals bubbles between the cell metallization and the lamination material in the EVA based test modules directly after lamination. They grow during the first 125 h damp heat test and become more flat afterwards. The Tectosil silicon elastomer shows no bubbles after lamination and for the complete testing duration of 2000 h. Laminate C ("open" sample) is used for the visual inspection of the solder joints and the metallization. The metallic rear side of the samples, shown in Fig.6, darkens during the damp heat test in three forms of appearance. Especially the flux with the high solid content (959T) darkens the metallization around the solder joints already during soldering. Small, dark spots are distributed randomly over the metallized area after 125 h damp heat test. The whole area begins to darken after 500 h. It starts at the metallization edges and after 1000 h to 2000 h the whole metallization is dark.

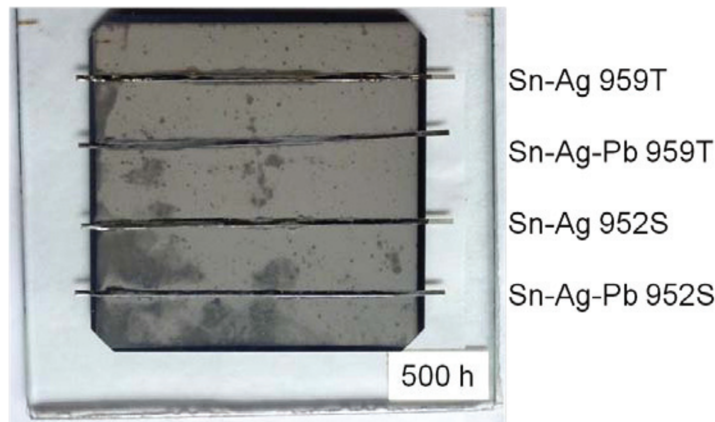

Fig. 6. Laminated sample for visual inspection after 500 h of damp heat test with four tested solder/flux combinations on the samples. Darkening around the solder joints, randomly distributed dark spots and whole area darkening, beginning at the edges, can be seen.

Fig. 7 shows the normalized contact resistivities (RC/RC.in) as a function of the damp heat test duration. There is no significant increase in the normalized contact resistivities for Sn-Ag/959T solder joints in a laminate type C ("open" sample). We got similar results for all solder/flux combinations in the "open" sample and the Tectosil laminates. In the EVA laminate RC/RC.in is constant for 1000 h damp heat for all solder flux combinations. During the damp heat test no connector fails.

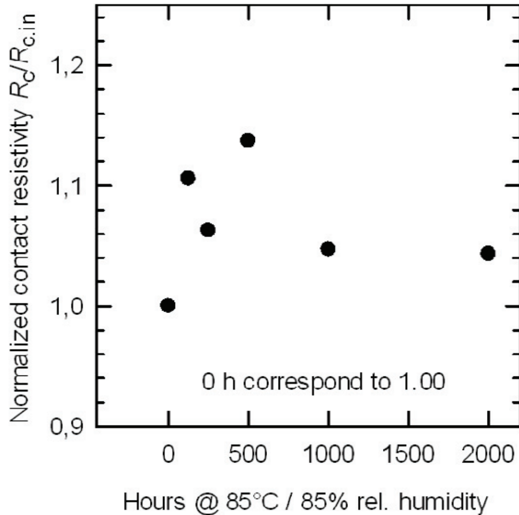

Fig. 7. Mean deviation of the normalized contact resistivity plotted as a function of the testing duration for the solder/flux combination Sn-Ag/959T in an "open" sample laminate.

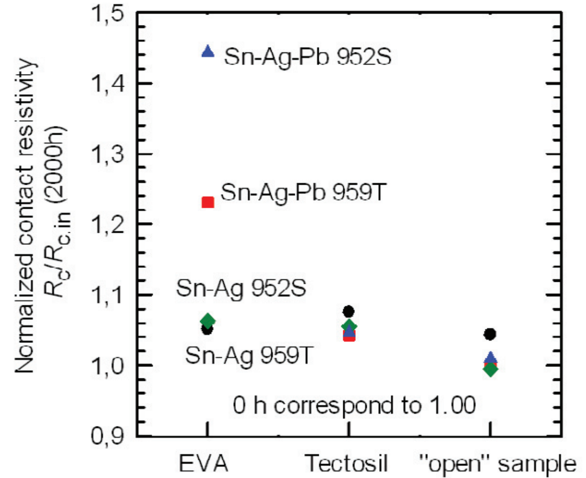

Fig. 8. Mean deviation of the normalized contact resistivity for four solder/flux combinations in different laminates after 2000 h of damp heat test.

In Fig. 8 the mean deviation of $R_C/R_{C.in}$ after 2000 h damp heat is shown as function of the solder, the flux and the lamination material. As can be seen $R_C/R_{C.in}$ in the laminates type B and C is about 1.00 – 1.08 after 2000 h damp heat for all solder and flux combinations and thus almost constant. That also applies to the Sn-Ag solders in the type A laminate. In contrast $R_C/R_{C.in}$ of the Sn-Ag-Pb solders increases up to 1.45. Thus a combination of a lead-containing solder in a laminate type A is the least stable combination.

4. Discussion and Conclusion

The solderability of the metallization stack is demonstrated not only as prepared, but also after accelerated storage and after half a year storage at room temperature by performing a 180° peel test. The lead-free Sn-Ag solders show the highest and most stable peel force without a dependance on the flux. The lead-containing solders reveal much lower peel forces nearby or smaller than the threshold of 1 N/mm and to some extent, especially in combination with the low solid content flux, fail the peel test. Due to similar results in accelerated storage and half a year storage the accelerated storage test can be applied to test the storage stability of similar metallization stacks in the future. As the adhesion fracture is always in the solder an adequate adhesion of the different metal layers is demonstrated.

A darkening of the metallization is seen during a damp heat test for 2000 h in the EVA laminates without back sheet in three forms of appearance. First, a darkening around the solder joints prepared with the high solid content flux appears directly after soldering. Second, dark spots which may be caused by impurities on the metal surface emerge after 125 hours damp heat. Possible sources of these impurities are flux spots. Third, a darkening of the total area starting at the metallization edges appears. This is the most reactive position of the metallization as here all three metal surfaces are located next to each other. A start of a chemical reaction is here most probable. In spite of all visual effects, no connector fails within 2000 h testing duration.

In the Tectosil laminate, the "open" laminate and the lead-free solders in the EVA laminate the normalized contact resistivity does not show a significant change within 2000 h damp heat test. Only the normalized contact resistivity for the lead-containing solders in the EVA laminate increases after 2000 h damp heat. Presumably that is caused by the bubbles and therewith in adhesion problems of the EVA foil and the metallization. We also checked if the appearance of the bubbles is caused by the special EVA. But repeating the same test with a new fresh EVA of another supplier reveals the same bubbles. Hence the application of EVA is potentially critical in particular in combination with lead-containing solders on an Al/Ni:V/Ag metallization stack. The test modules with the Tectosil silicone elastomer show a smaller increase in the normalized contact resistivity and no bubbles abounded. The silicone elastomer may be more convenient than the EVA foil for laminating this metallization stack.

In summary the favored and most stable solder, flux and lamination material combination to form a long term stable solder joint on an Al/Ni:V/Ag metallization is a lead-free Sn-Ag connector soldered with the low solid content flux in a silicone elastomer based laminate.

Acknowledgements

The authors would like to thank Sven Schramm from Applied Materials GmbH, Alzenau, for preparing the metallization layers. Funding was provided by the State of Lower Saxony and the German Ministry for the Environment, Nature Conservation and Nuclear Safety (BMU) under Contract No. 0325195A (VaCoC).

References

[1] T. Dullweber, S. Gatz, T. Falcon, and H. Hannebauer, High efficiency rear-passivated screen-printed silicon solar cells, *Photovoltaics International*, Vol. 13, pp. 81-7, 2011.

[2] C. Mader, M. Kessler, U. Eitner, and R. Brendel, Temperature of silicon wafers during in-line high-rate evaporation of Aluminum, *Sol. Energy Mater. Sol. Cells*, vol. 95, no. 11, pp. 3047-53, 2011, doi:10.1016/j.solmat.2011.06.031.

[3] F. Heinemeyer, C. Mader, D. Münster, T. Dullweber, N.P. Harder, and R. Brendel, Inline high-rate thermal evaporation of Aluminum as a novel industrial solar cell metallization scheme, *Proc. 2nd Workshop on Metallization*, Constance, Germany 2010, pp. 48-51.

[4] J. Nekarda, D. Reinwand, A. Grohe, P. Hartmann, R. Preu, R. Trassl, and S. Wieder, Industrial PVD metallisation for high efficiency crystalline silicon solar cells, *34th IEEE Potovoltaic Specialists Conference (PVSC)*, Philadelphia, USA, 2009

[5] V.Jung, M. Köntges, Al/Ni:V/Ag metal stacks as rear-side metallization for crystalline silicon solar cells, *Prog. Photovolt: Res. Appl.*, 2012, DOI: 10.1002/pip.2169.

[6] J. Osenbach, A. Amin, M. Bachman, F. Baiocchi, D. Bitting, D. Crouthamel, et.al., Stability of flip-chip interconnects assembled with Al/Ni(V)/Cu-UBM and eutectic Pb-Sn solder during exposure to high-temperature storage, *J. Electron. Mater.*, vol. 38, no. 2, pp. 303 – 24, 2009.

[7] G.Y. Jang, J.G. Duh, Elemental redistribution and interfacial reaction mechanism for the flip chip Sn-3.0Ag-(0.5 or 1.5)Cu solder bump with Al/Ni(V)/Cu under-bump metallisation during aging, *J. Electron. Mater.*, vol. 35, no. 11, pp. 2061-70, 2006.

[8] W.J. Choi, E.C.C. Yeh, K.N. Tu, Mean-time-to-failure study of flip chip solder joints on Cu/Ni(V)/Al thin-film under-bump-metallization, *J. Appl. Phys.*, vol. 94, no. 9, pp. 5665-71, 2003.

[9] U. Eitner, M. Köntges, and R. Brendel, Use of digital image correlation technique to determine thermomechanical deformations in photovoltaic laminates: Measurements and accuracy, *Sol. Energy Mater. Sol. Cells*, vol. 94, pp. 1346-51, 2010, doi:10.1016/j.solmat.2010.03.028.